ACCSCIENCE PUBLISHING

Materials Science in Additive Manufacturing

ORIGINAL RESEARCH ARTICLE

Disinfection efficiency and its impact on the mechanical properties of multi-material mouthguards fabricated via fused filament fabrication

Leonor Bispo, Joana F. Henriques, Ana P. Piedade*, and Ana M. Sousa

Department of Mechanical Engineering, CEMMPRE, University of Coimbra, 3030-788 Coimbra, Portugal

Abstract

Mouthguards are orthodontic devices designed to prevent orofacial injuries during sports activities. To ensure comfort and correct positioning, they must fit the athlete's dental arch precisely. Customization through additive manufacturing offers a practical solution for producing well-fitted mouthguards. The present study aimed to investigate the use of 3D-printed multi-material parts in the fabrication of protective mouthguards. Three polymeric materials were employed: High-impact polystyrene (HIPS), thermoplastic polyurethane, and poly(methyl methacrylate) (PMMA). Two configurations – bi-layered and tri-layered – were analyzed to assess the influence of material arrangement on mechanical performance. The impact of disinfection methods on mechanical properties was also evaluated, comparing physical (ultraviolet [UV]-C light exposure) and chemical (Polident cleaning tablet solution) disinfection strategies. In addition, the effects of artificial saliva aging on all material types and configurations were examined. Mechanical testing revealed that multi-material configurations containing HIPS exhibited superior mechanical performance, with flexural stiffness values 8 – 40% higher than PMMA-based samples, Vickers microhardness 40 – 128% greater, and absorbed energy and impact strength improved by 11 – 105%. Moreover, the tri-layered configuration demonstrated enhanced mechanical behavior, showing approximately 40% higher transverse impact resistance and increases of ~35% and ~77% in flexural strength and modulus, respectively, relative to the bi-layered configuration. Disinfection studies confirmed the efficacy of both approaches, reducing *Staphylococcus aureus* colony-forming units by 95% (Polident) and 97% (UVC light). These findings are promising for the development of protective mouthguards, where changes in mechanical properties over time – particularly due to saliva exposure and disinfection – are of critical importance.

Keywords: Mouthguards; Multi-material configuration; Disinfection; Material characterization; Additive manufacturing

***Corresponding author:**
Ana Piedade
(ana.piedade@dem.uc.pt)

Citation: Bispo L, Henriques JF, Piedade AP, Sousa AM. Disinfection efficiency and its impact on the mechanical properties of multi-material mouthguards fabricated via fused filament fabrication. *Mater Sci Add Manuf.* 2025;4(2):025130018. doi: 10.36922/MSAM025130018

Received: March 28, 2025

Revised: April 13, 2025

Accepted: April 22, 2025

Published online: May 20, 2025

1. Introduction

Orofacial injuries are common in contact sports, where athletes are frequently exposed to high-impact forces. Sports such as boxing, rugby, karate, wrestling, and hockey are

particularly associated with severe dental fractures and soft tissue traumas,[1] which may lead to more serious complications, such as mandibular fractures and facial bone fractures, even irreversible brain damage.[2,3]

Since 1960, the American Dental Association (ADA) has recommended the use of mouthguards across a range of sports to reduce the incidence of such injuries.[4] According to the American Society for Testing and Materials (ASTM), a mouthguard is defined as a "sturdy device or appliance placed inside the mouth to reduce oral injuries, particularly to the teeth and surrounding structures."[5] An effective mouthguard should fit the athlete's dental arch precisely, cause minimal discomfort, and provide protection against impact-related injuries to the teeth and surrounding tissues during contact sports.[6,7]

Following ADA guidelines, mouthguards are classified into three categories: Extraoral, intraoral, and combined types.[8] Intraoral mouthguards are further subclassified based on their manufacturing method into three categories: Stock, "boil and bite," and custom-made mouthguards.[8]

Stock protective devices (type I) are commercially available in standardized sizes at affordable prices. However, their inability to conform to the athlete's oral anatomy compromises their functionality, reducing their ability to absorb and dissipate impact energy effectively. These devices may also create a false sense of security and are often associated with discomfort, including nausea and respiratory difficulty.[6,9]

"Boil and bite" mouthguards (type II) are an improved version of type I mouthguards. Made from thermoplastic polymers,[10] they can be softened in hot water and molded to the user's teeth and oral tissues.[6] While they offer better adaptation than stock mouthguards, they do not provide a fully customized fit and may still cause discomfort, as well as difficulty breathing or speaking during use.[11] With repeated use, there is a significant risk of dental damage, particularly to the most prominent teeth, due to the progressive reduction in thickness from wear. This degradation compromises the device's ability to provide effective orofacial protection.[6,9,12]

Custom-made mouthguards (type III) are fabricated to offer superior fit and alignment with the athlete's dental arch, thereby enhancing intraoral stability and minimizing the risk of dislodgment and mechanical failure.[9] However, these devices must be custom-manufactured and require at least one dental consultation, resulting in a significantly higher cost compared to types I and II.[6,9,12]

Currently, most custom-made mouthguards are produced using thermoforming technologies, encompassing both pressure and vacuum thermoforming methods.[6,13] These manufacturing strategies typically use 4 mm-thick sheets of the copolymer poly(ethylene-vinyl acetate) (EVA), which are heated and molded over a cast of the athlete's dentition.[6,14] EVA is favored for its impact resistance and favorable mechanical and physical properties. However, its relatively low rigidity and hardness limit its energy dissipation capacity.[15] Moreover, EVA is prone to swelling, which can lead to dimensional and geometrical instability, including increased thickness. In addition, issues related to microbial adhesion have been reported.[16]

Conventional manufacturing techniques also involve multiple production stages and generate considerable material waste, raising concerns about the environmental sustainability of mouthguard fabrication. To address these limitations, additive manufacturing has been investigated as an alternative production method.[6,11,17] In particular, fused filament fabrication (FFF) is considered a more sustainable approach, as it eliminates the need for molds and minimizes material waste.[6] As such, FFF presents a viable strategy for producing protective mouthguards that are more closely tailored to the athlete's dental arch.

Nonetheless, several challenges hinder the application of FFF in dentistry, including fiber orientation, weak interfacial bonding between the fiber and matrix, and void formation. Multi-material 3D printing, however, offers a promising solution by integrating materials with distinct mechanical and physical properties. This approach enhances the overall mechanical performance of printed components and enables the introduction of novel functionalities.[18] In the context of mouthguard development, it soon became evident that the standard 4 mm thickness of commercially available devices posed a major obstacle for athletes. Reducing the thickness of these devices emerged as a critical design goal. However, this seemingly straightforward objective could not be achieved using monolithic materials such as EVA, which is currently the material of choice for conventional mouthguards. This limitation underpins the rationale for adopting a multi-material approach. By combining rigid and soft materials – offering mechanical strength and impact energy absorption, respectively – this strategy has been shown to improve protective performance, as demonstrated in previous studies.[18,19]

In addition to mechanical performance, the correct disinfection of mouthguards is crucial for safeguarding athletes' health. Due to the high microbial load of the oral cavity, it is essential to disinfect these devices after each use to minimize contamination risk and prevent illness, similar to hygiene protocols in clinical settings.[20,21]

Despite the favorable results related to mouthguard hygiene, standardized guidelines for optimal disinfection

practices and appropriate disinfection agents are still lacking.[22,23] Furthermore, few studies have investigated how disinfection strategies affect the mechanical performance of mouthguards. Existing disinfection and sterilization methods include ultrasonic cleaning[24] and the use of commercially available cleaning tablets, such as Corega, Fittydent, and Polident.[22,23]

Therefore, the present work aimed to develop multi-material mouthguards using FFF technology, incorporating thermoplastic polyurethane (TPU) as the soft material and high-impact polystyrene (HIPS) and poly(methyl methacrylate) (PMMA) as rigid materials. Two material configurations were assessed, namely a sandwich-like tri-layered configuration and a bi-layered configuration. The choice of materials was based on previous research.[19] Mechanical performance was assessed through three-point bending tests and transverse impact tests to evaluate flexural and impact resistance, respectively. A novel aspect of the current work is the investigation of the effects of artificial saliva aging and disinfection procedures – both physical (ultraviolet [UV]-C light) and chemical (cleaning tablet solution) – on the mechanical properties of the multi-material mouthguards.

2. Materials and methods

2.1. Materials

The present study examined three commercially available polymeric filaments (Ø = 1.75 ± 0.04 mm), used without further modifications: PMMA, purchased from TreeD Filaments (Italy); TPU, commercially labeled as Traffic Black, acquired from BeeVeryCreative (Portugal); and HIPS, supplied by DoWire (Portugal). As previously stated, the selection of these materials was based on previous studies conducted by the authors,[19] particularly considering their performance in energy absorption and dissipation during impact testing. These characteristics supported the inclusion of the three polymers evaluated in this study. Additionally, 4 mm-thick bulk EVA specimens were acquired from Dentaflux (Spain) to compare the mechanical properties of conventional mouthguard materials with those fabricated via 3D printing.

Thermoplastic polyurethanes are good shock absorbers and easy to process, making them promising candidates for mouthguard manufacturing and potential substitutes for EVA. However, the issue of excessive mouthguard thickness remains unsolved, as both TPU and EVA are elastomeric polymers with relatively low impact strength. To address this limitation, a multi-material strategy was employed, combining impact-resistant materials such as PMMA or HIPS with TPU to reduce the overall device thickness. Both PMMA and HIPS are widely available, cost-effective, and easily processed through FFF.[25,26] Table 1 summarizes the properties and selected biomedical applications of HIPS, TPU, and PMMA.

To simulate an intraoral environment, all specimens were soaked in artificial saliva prepared following the Fusayama–Meyer formulation (Table 2), in compliance with ISO 10271.[24] Potassium chloride, sodium chloride, calcium chloride dihydrate, monosodium phosphate, and urea were obtained from Panreac (Spain), whereas sodium sulfate monohydrate was purchased from Sigma-Aldrich (Germany).

2.2. Chemical characterization of the filaments

Fourier transform infrared (FTIR) spectroscopy was used to validate the chemical composition of the filaments and to detect any potential chemical modifications following disinfection procedures. The analysis was conducted using a Bruker Alpha II spectrometer (mid-infrared: 4000 – 400 cm^{-1}; Bruker, United States), equipped with an RTDLATGS detector (Bruker, United States) and a KBr beam splitter (Bruker, United States). Spectra were recorded at room temperature with a

Table 1. Properties and biomedical applications of HIPS, TPU, and PMMA

Material	Properties and characteristics	Biomedical applications	References
High-impact polystyrene (HIPS)	Dimensional stability, compatibility with radiation sterilization, high impact strength. More ductile than polystyrene due to the addition of an elastomer to the polymer backbone, while maintaining equivalent cytocompatibility.	Catheter trays, heart pump trays, epidural trays, respiratory care equipment, syringe hubs, suction canisters, and bone replacements.	27,28
Thermoplastic polyurethane (TPU)	Combines flexibility (soft segments) and stiffness (hard segments); chemical stability; good lubricity and abrasion resistance; elastomeric behavior; high shock absorption capacity.	Blood bags, heart valves, vascular grafts, long- and short-term implants, and cardiac pumps.	29,30
Poly (methyl methacrylate) (PMMA)	Good optical properties; long-term mechanical stability; high impact strength; lightweight; shatter-, weather-, and scratch-resistant.	Bone cement, intraocular lenses, artificial corneal implants (keratoprosthesis), bone substitutes, and mandibular reconstruction.	31,32

resolution of 4.0 cm^{-1}, using 24 accumulations and a constant applied force across all acquisitions.

2.3. Fabrication and disinfection procedures

2.3.1. 3D printing

All testing specimens were prepared using FFF technology with a FlashForge™ Creator3 3D printer (Filament2Print, Spain), equipped with a dual extruder, each fitted with a 0.4 mm diameter nozzle. Specimens were printed with a layer height of 0.1 mm and a printing speed of 40 mm/s. A 100% line infill with a -45°/45° orientation was applied to all parts to ensure uniform stress distribution and reduced anisotropic mechanical behavior.[11,17]

Two multi-material configurations were studied, as depicted in Figure 1. The tri-layered configuration (Figure 1A) comprised a TPU core with outer sections of either PMMA or HIPS, each accounting for one-third of the total specimen height. In contrast, the bi-layered configuration (Figure 1B) was composed of a TPU base (half of the total height) followed by PMMA or HIPS forming the upper half. The selection of printing temperatures, bed temperatures, and materials was based on the authors' previous research.[19] The printing parameters used in the present work are summarized in Table 3.

It is worth noting that multi-material 3D printing presents inherent challenges, particularly regarding interfacial adhesion – a subject extensively addressed by other researchers.[33]

Table 2. Composition of Fusayama–Meyer artificial saliva

Component	Concentration (g/L)
Potassium chloride	0.4
Sodium chloride	0.4
Calcium chloride dihydrate	0.906
Monosodium phosphate	0.69
Sodium sulfide nonahydrate	0.005
Urea	1.0

Notes: The solution was prepared using Milli-Q water according to the protocol stated in Hayashi *et al.*[23]

The resulting multi-material configurations are depicted in Figure 2. The 3D-printed parts exhibit a parallelepipedal geometry with dimensions of 60 × 10 × 2 mm3. The printed specimens demonstrated dimensional consistency, with a standard deviation of approximately 0.1 mm.

2.3.2. Disinfection of 3D-printed components

Proper cleaning and disinfection of mouthguards are essential for the health and well-being of athletes. Accordingly, two disinfection methods were tested: a chemical approach using commercially available cleaning tablets (Polident) and a physical approach using UVC irradiation (λ = 254 nm; Germix SM-504B, Amazon EU, Luxembourg).

Prior to disinfection, 3D-printed specimens were individually immersed in artificial saliva for 2 h at 37°C and 100 rpm (using a Gerhardt THO 500/1 incubator shaker [Gravimeta, Portugal]). The chemical disinfection was performed by immersing specimens in a Polident solution (0.02 g/mL in Milli-Q water) for 5 min;[23] these were subsequently referred to as post-Polident specimens. The physical disinfection involved irradiating pre-dried specimens for approximately 45 min under UVC light (referred to as post-UVC specimens).

This soaking-disinfection process was repeated cyclically until a total of 36 h of immersion (18 cycles) was completed, simulating cumulative exposure equivalent to 3 months of typical device use. Figure 3 depicts a schematic of the disinfection protocol.

Dry, untreated samples from each multi-material configuration served as negative controls. Specimens that underwent immersion in artificial saliva but were not disinfected were considered positive controls (hereafter, pre-disinfected specimens).

2.4. Assessment of disinfection effectiveness

The effectiveness of the disinfection procedures was assessed by quantifying the number of *Staphylococcus aureus* colony-forming units (CFUs) that developed on the surfaces of the specimens following chemical (Polident

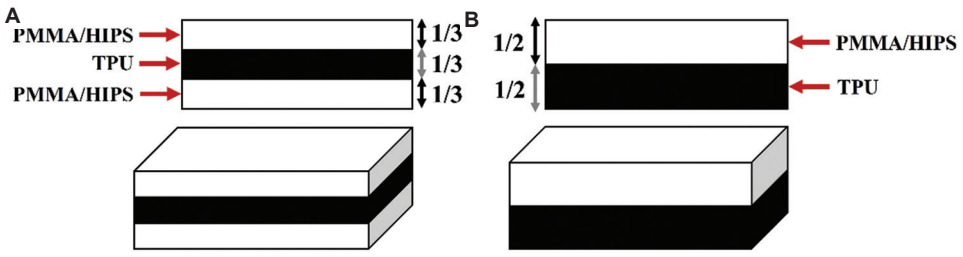

Figure 1. Configuration of the 3D-printed structures. (A) Tri-layered and (B) bi-layered arrangements
Abbreviations: HIPS: High-impact polystyrene; PMMA: Poly(methyl methacrylate); TPU: Thermoplastic polyurethane

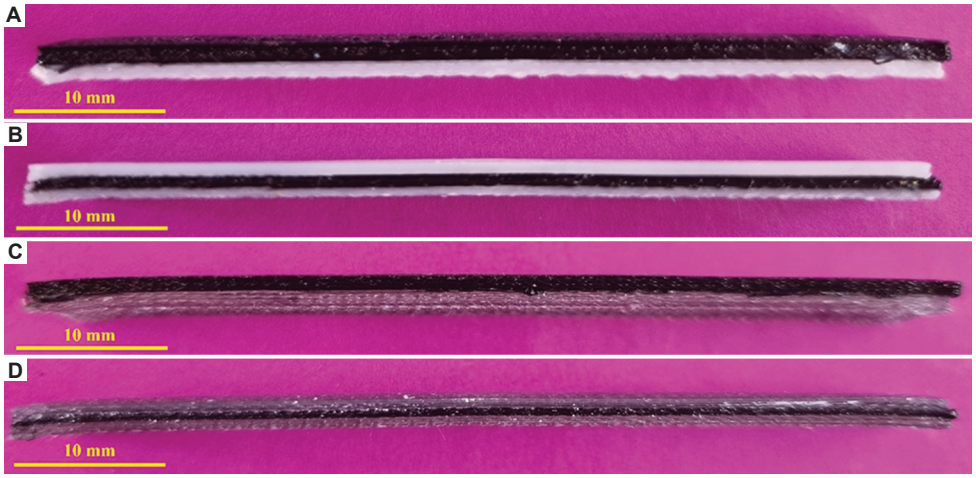

Figure 2. Multi-material parts after 3D printing, using high-impact polystyrene and thermoplastic polyurethane (TPU)—(A) bi-layered and (B) tri-layered configurations; and poly(methyl methacrylate) and TPU—(C) bi-layered and (D) tri-layered configurations. Scale bars: 10 mm

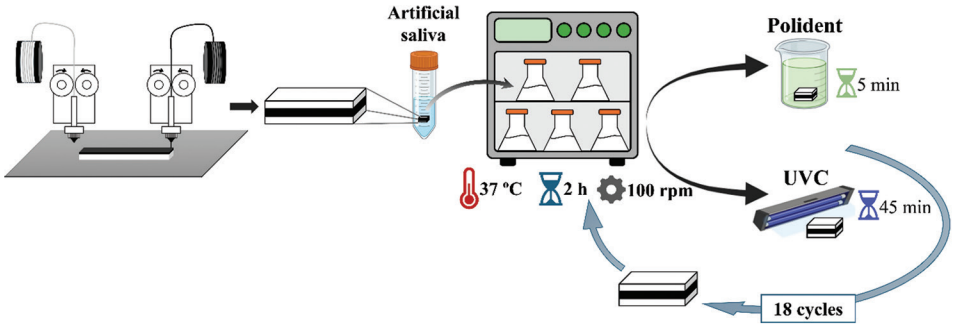

Figure 3. Schematic representation of the disinfection methodology applied to the 3D-printed surfaces

Table 3. Printing parameters of the 3D-printed specimens

Configuration	Arrangement	T_{bed} (°C)	Filament	$T_{printing}$ (°C)
Tri-layered configuration	PMMA-TPU-PMMA	90	TPU	230
			PMMA	240
	HIPS-TPU-HIPS	90	TPU	230
			HIPS	240
Bi-layered configuration	TPU-PMMA	40	TPU	230
			PMMA	240
	TPU-HIPS	40	TPU	230
			HIPS	240

Notes: T_{bed}: Bed temperature; $T_{printing}$: Printing temperature.
Abbreviations: HIPS: High-impact polystyrene; PMMA: Poly (methyl methacrylate); TPU: Thermoplastic polyurethane.

immersion for 5 min) or physical (irradiated with UVC light for 45 min) disinfection.

To simulate mouthguard contamination during use, specimens were first inoculated with *S. aureus* (~10^8 cells/mL) and incubated at 37°C for 1 h. They were then subjected to one of the two disinfection methods. After disinfection, the specimens were incubated at 37°C for an additional 24 h to promote bacterial colony growth. CFUs were counted at the end of this incubation period. Non-disinfected specimens served as controls. The disinfection effectiveness was determined by comparing the CFU counts between disinfected and control groups.

2.5. Post-processing characterization

2.5.1. Mechanical characterization

To evaluate the flexural mechanical properties of the multi-material specimens (60 × 10 × 2 mm^3), a three-point bending test was conducted using a Shimadzu Autograph AGS-X Universal Testing Machine (Shimadzu, Japan) equipped with a 5 kN load cell, operating at a test speed of 2 mm/min. Flexural strength (σ_f) and flexural modulus (E_f) were determined for each configuration and treatment condition following the ASTM D790 standard recommendations.[34]

The calculations followed established procedures described in prior studies.[11] Specifically, σ_f was calculated at the mid-span using the maximum nominal bending stress, as shown in Equation I:

$$\sigma_f = \frac{3P_{máx}L}{2bh^2} \quad \text{(I)}$$

Where P is the applied load, L is the span length, b is the specimen width, and h is the specimen thickness.[35] The flexural modulus, E_f was determined using the theory of linear elastic bending beams, according to Equation II:

$$E_f = \frac{\Delta P L^3}{48 \Delta \mu I} \quad \text{(II)}$$

Where I is the moment of inertia of the cross-section, and ΔP and $\Delta \mu$ are the load range and flexural displacement range, respectively, within the linear region of the load-displacement curve.[36] All results are presented as the mean ± standard deviation of the mean value. For comparison, bulk EVA specimens (90 × 10 × 4 mm^3), the standard material for mouthguard fabrication, were also tested.

Given the functional demand placed on mouthguards, transverse impact tests were conducted to further characterize the mechanical resilience of the 3D-printed parts. Charpy impact tests were performed using V-shaped notched specimens (80 × 10 × 2 mm^3, with a 1 mm V-notch) in accordance with the ISO 179 standard.[37] These tests assessed the energy absorbed during impact to determine the impact resilience of the materials.

Impact testing was conducted at room temperature (~20°C) using a Ceast 9050 impact machine (Instron, United States) equipped with a 5 J hammer set at a 150° release angle. For each configuration (tri-layered and bi-layered) and post-processing treatment (dry, pre-disinfected, post-Polident, and post-UVC), triplicate samples were evaluated. Control tests were also conducted on bulk EVA specimens (80 × 10 × 4 mm^3).

2.5.2. Surface characterization

Vickers microhardness testing was conducted to assess the surface mechanical properties of the 3D-printed specimens. Given that disinfection treatments primarily affect the outermost polymer chains, it is essential to assess the influence of UVC irradiation and Polident immersion on surface-level mechanical properties.

Microhardness was measured using Duramin DK 2750 version 0.04 (Eqpolymers, Denmark), equipped with a Vickers indenter, in accordance with ISO 6507.[38] For each material configuration (bi-layered and tri-layer) and treatment condition (dry, pre-disinfected, post-Polident, and post-UVC), three specimens were analyzed. Each specimen underwent three indentations using a 490 mN load and a holding time of 15 s.

Surface topography was assessed using a fringe projection phase-shifting method with the Attention 3D Topography Module integrated into the Theta Flex optical tensiometer (Biolin Scientific, Sweden). Key surface roughness parameters were measured, including the *r factor* (defined as the ratio of the true surface area to the projected area), the average surface roughness (S_a), and the quadratic surface roughness (S_q) were determined.

Wettability was assessed by measuring the static contact angle of Milli-Q water at room temperature using the Theta Flex optical tensiometer. For each specimen, five drops (5 μL each) were deposited, and the contact angles were recorded once the air–water–surface interface reached equilibrium (θ_a). Contact angle correction for surface roughness was applied using Wenzel's equation (Equation III):

$$Cos\theta_a = r \times cos\theta_r \quad \text{(III)}$$

Where θ_r is the corrected angle for a smooth surface, θ_a is the measured contact angle, and r is the roughness factor obtained from the topography analysis.[39]

3. Results

3.1. Chemical characterization

FTIR spectroscopy analysis was conducted to identify the characteristic chemical functional groups of each polymeric filament and to confirm their chemical composition (fingerprint). The spectra of each filament before 3D printing are present in Figure 4.

The spectra exhibit the expected vibrational bands characteristic of each polymeric material. For TPU (Figure 4A), the following vibrations were identified: C–N stretching at 1220 cm^{-1},[40] N–H bending at 1527 cm^{-1},[41] and C=O stretching at 1729 cm^{-1},[40] associated with the urethane linkage. Additionally, bands centered at 1000 and 1075 cm^{-1} correspond to asymmetric stretching of C–O–C groups from polyether and urethane segments, respectively.[42]

In the spectrum of HIPS (Figure 4B), a broad band between 3200 and 3000 cm^{-1} is attributed to aromatic C–H stretching.[43] Vibrations associated with C=C stretching in the benzene ring were observed at 1601, 1490, and 1446 cm^{-1},[43,44] while CH_2 stretching appeared at 2920 cm^{-1}.[45] Intense bands at 752 and 693 cm^{-1} confirm the presence of monosubstituted benzene rings, in agreement with previous studies.[35] For PMMA (Figure 4C), the stretching frequencies of O–CH_3, C=O, and CH_2 groups were observed at 986 cm^{-1},[46] 1723 cm^{-1},[47] and 2951 cm^{-1},[48]

respectively. An asymmetric stretching peak at 1143 cm^{-1}, corresponding to the C–O–C group, was also noted.[49]

Comparison with reference spectra from the literature suggests that any additives or potential contaminants present do not significantly alter the overall chemical composition of the investigated materials.

Moreover, FTIR spectra were recorded after the specimens underwent disinfection treatments—either UVC irradiation or immersion in Polident solution—to assess potential chemical modifications in their structures by these processes. The characterization was performed immediately after the disinfection procedures for all three materials (Figure 5).

When compared to the spectra of untreated (dry state) specimens, the main vibrational bands corresponding to

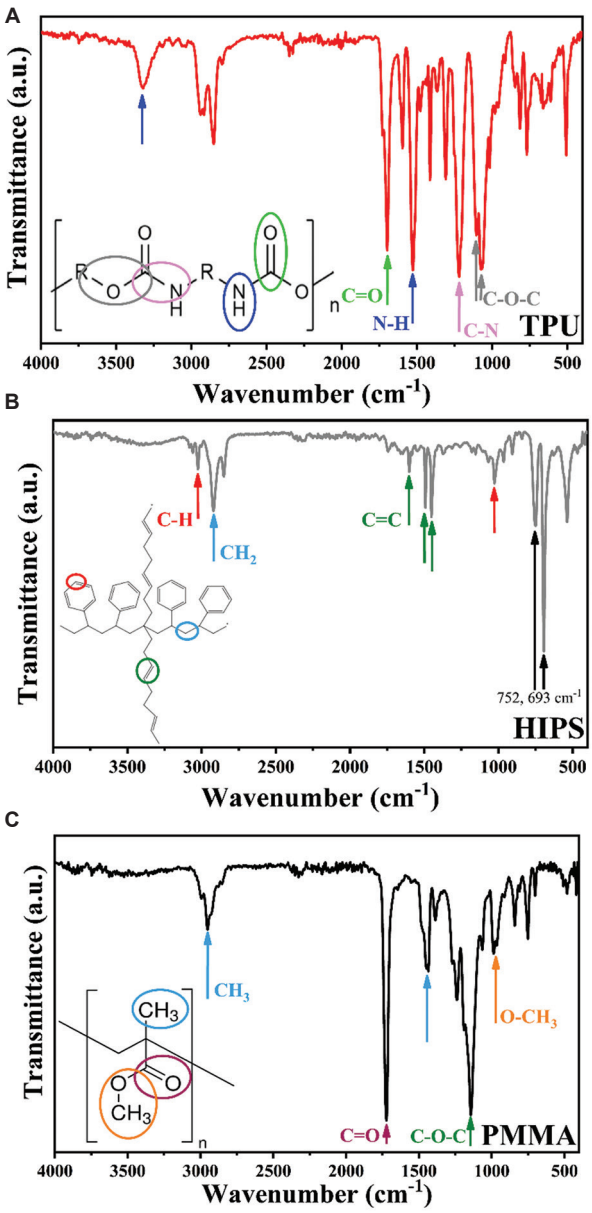

Figure 4. Fourier transform infrared spectra of the studied polymeric filaments: (A) thermoplastic polyurethane (TPU), (B) high-impact polystyrene (HIPS), and (C) poly(methyl methacrylate) (PMMA). Key functional groups are indicated in each spectrum

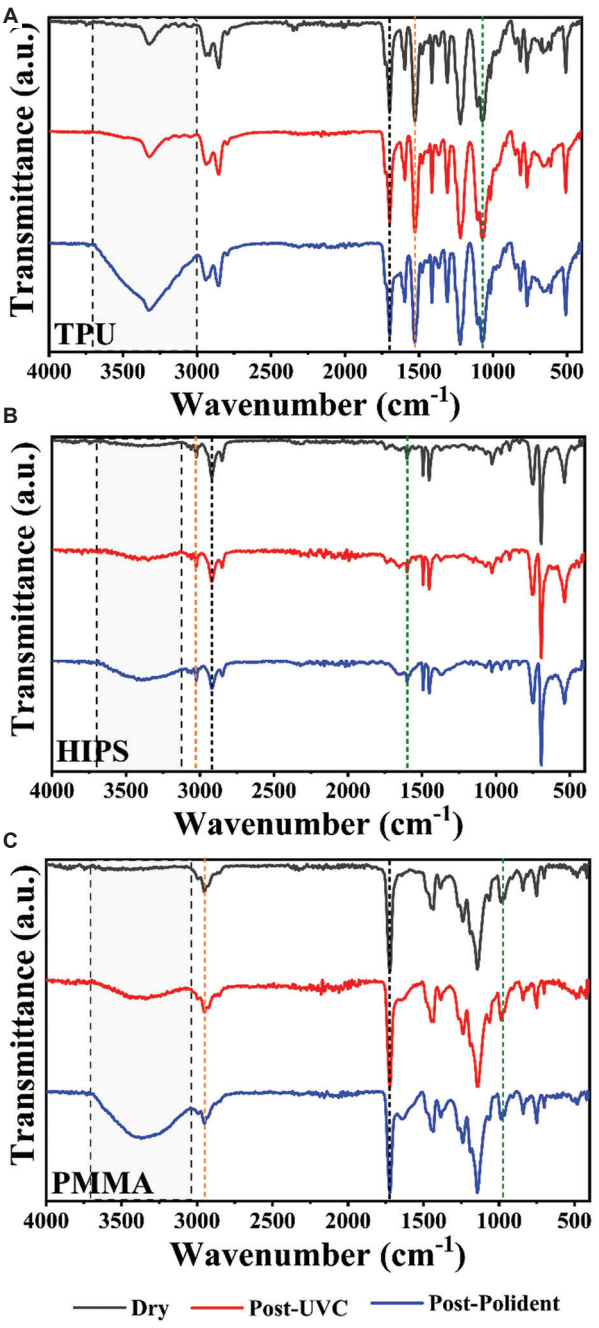

Figure 5. Fourier transform infrared spectra of polymeric materials following disinfection: UVC radiation (red) and Polident immersion (blue), for (A) thermoplastic polyurethane (TPU), (B) high-impact polystyrene (HIPS), and (C) poly(methyl methacrylate) (PMMA)

functional groups remained largely unchanged. However, a broad band centered around 3400 cm^{-1}, corresponding to hydroxyl groups (-OH), emerged after disinfection, indicating minor chemical modifications. This band was more pronounced in post-Polident specimens, likely due to the aqueous nature of the cleaning tablet solution. In contrast, the presence of the -OH band in post-UVC specimens may result from the formation of oxygen radicals upon irradiation, which subsequently react with hydrogen radicals to form hydroxyl groups.[47]

3.2. Assessment of disinfection effectiveness

The effectiveness of the disinfection protocols was evaluated by counting CFUs after a 24-h incubation period on disinfected surfaces.[50] The number of CFUs was higher in post-Polident specimens (9 ± 1 CFUs) than in post-UVC specimens (4 ± 1 CFUs). Given the overall low CFU counts observed in the Petri dishes, bacterial proliferation was considered negligible. These results indicate that both disinfection protocols are effective for disinfecting mouthguards (Figure 6). However, UVC disinfection appears to be the more viable option, offering greater economic and environmental sustainability over the long term.

3.3. Mechanical characterization

3.3.1. Three-point bending test

Three-point bending tests were conducted to determine the flexural modulus (E_f) and flexural strength (σ_f)[34] of each multi-material configuration (Figure 7). Furthermore, the

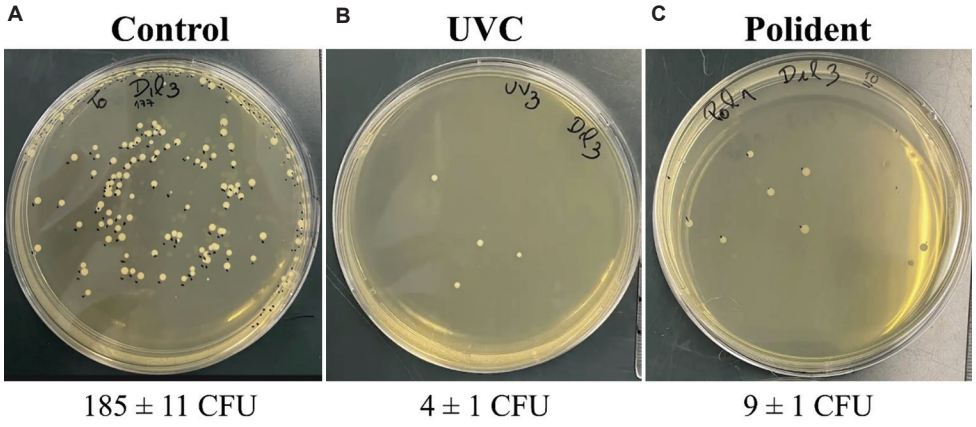

Figure 6. Assessment of disinfection effectiveness, with lower colony-forming unit counts indicating greater efficacy. (A) Control; (B) post-Polident specimen; (C) post-UVC specimen

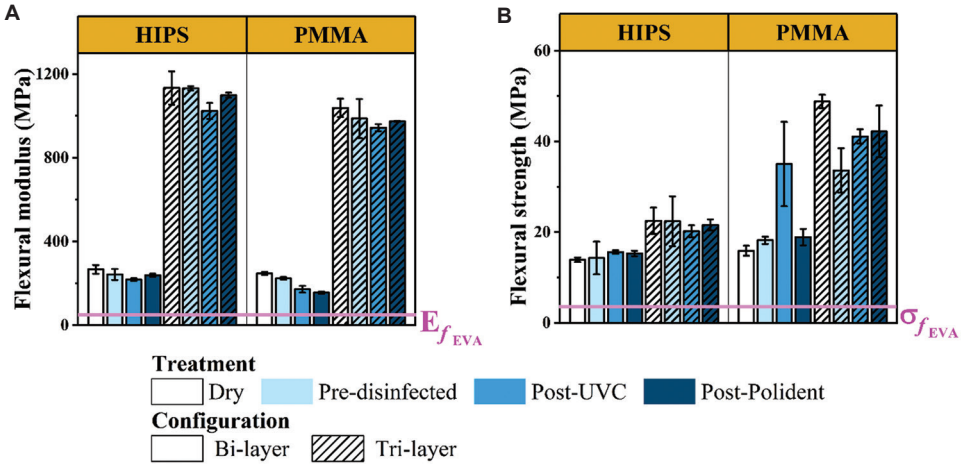

Figure 7. Flexural mechanical properties of multi-material 3D-printed components as determined through three-point bending tests. (A) Flexural modulus and (B) flexural strength for bi-layered and tri-layered configurations after UVC exposure or Polident immersion. The pre-disinfected group refers to specimens immersed in artificial saliva without subsequent treatment. For reference, bulk poly(ethylene-vinyl acetate) (EVA; pink) exhibited E_f = 35.8 ± 2.2 MPa and σ_f = 1.4 ± 0.1 MPa
Abbreviations: HIPS: High-impact polystyrene; PMMA: Poly(methyl methacrylate); TPU: Thermoplastic polyurethane

impact of disinfection treatments on these properties was assessed.

Since mouthguard materials must absorb, dissipate, and redistribute impact energy across a broader area, they require sufficient rigidity under load.[11] As reported by Cummins and Spears,[51] stiffer materials are generally more effective at energy dissipation and stress redistribution. Accordingly, a higher E_f value indicates a stiffer material.

Overall, specimens incorporating HIPS exhibited higher E_f values than those made with PMMA, aligning with literature findings that report superior stiffness in HIPS monomaterial samples.[11] The flexural properties of control specimens (dry and pre-disinfected) were broadly similar, likely due to minimal mass change during the aging process.

Concerning the effects of disinfection protocols on the mechanical properties of 3D-printed multi-material parts, both disinfection methods resulted in lower E_f values compared to control samples (dry and pre-disinfected). This reduction in mechanical characteristics was observed across both PMMA- and HIPS-based configurations.

In the case of chemical disinfection, two factors contribute to the decrease in flexural modulus:

(i) Chemical interactions between the constituents of the Polident solution and the polymer chains, which may reduce the average molecular weight and compromise mechanical integrity.
(ii) The presence of water is used to dissolve the cleaning tablet, which acts as a plasticizing agent and softens the polymer structure.

Meanwhile, UVC disinfection had the most pronounced adverse effect on the flexural modulus. The high-energy photons emitted during UVC exposure can cleave chemical bonds within the polymer chains, initiating a degradation process. This degradation process involves the formation of free radicals, which can react to form new chemical bonds, thereby altering the polymer's molecular structure and reducing mechanical stiffness.[17,52] Consequently, it can be surmised that disinfection adversely affects the rigidity of mouthguards, potentially impairing their ability to effectively dissipate and redistribute impact forces.

Moreover, across both material types, the tri-layered configuration exhibited higher E_f values compared to the bi-layered configuration, indicating superior impact energy dissipation due to greater overall rigidity. This is attributed to the higher relative content of TPU—a polymer with inherently low E_f[17]—in the bi-layered specimens compared to the tri-layered ones.

Finally, when comparing the materials and multi-material configurations under investigation with the most widely used mouthguard material (EVA), the 4 mm EVA specimens exhibited lower average values of both σ_f and E_f than the 2 mm 3D-printed specimens assessed in this study.

3.3.2. Charpy impact test

According to the ASTM F697-16,[5] mouthguards must be fabricated from resilient materials capable of absorbing, dissipating, and redistributing impact energy to prevent injuries to the teeth and surrounding oral structures. Accordingly, the samples were subjected to transverse impact testing,[37] and the results are presented in Figure 8.

Among the tested configurations, those incorporating HIPS exhibited the highest values for both impact strength (Figure 8A) and absorbed energy (Figure 8B). These findings are consistent with previous studies,[11,17] which have demonstrated that HIPS possesses superior impact resilience compared to PMMA.

Regarding the influence of multi-material configuration (bi- or tri-layer) and disinfection treatment on the transverse impact properties of HIPS- and PMMA-based 3D-printed parts, the results generally show no statistically significant differences. However, notable exceptions include:

- Bi-layered HIPS configurations, where a difference was observed between the dry-state condition (20.4 ± 0.6 $kJ \cdot m^{-2}$) and the post-Polident group (23.5 ± 2.5 $kJ \cdot m^{-2}$),
- Tri-layered HIPS configurations between disinfection conditions (21.1 ± 8.0 $kJ \cdot m^{-2}$ for post-UVC vs. 36.0 ± 2.3 $kJ \cdot m^{-2}$ for post-Polident), and
- Tri-layered PMMA configurations between disinfection groups (18.2 ± 1.2 $kJ \cdot m^{-2}$ for post-UVC vs. 26.3 ± 5.8 $kJ \cdot m^{-2}$ for post-Polident).

These findings suggest that the disinfection protocol can influence the transverse impact properties of 3D-printed parts, particularly in tri-layered configurations. Nevertheless, caution is warranted when interpreting these results due to the high standard deviations, which limit the statistical reliability of the conclusions.

An inspection of the damaged specimens following the Charpy impact test (Figure 9) revealed superior interfacial adhesion in tri-layer configurations compared to bi-layered ones. Clear separation at the material interface was frequently observed in the bi-layered specimens, which may explain the greater variability within these groups. As evidenced in the literature, premature cooling of the first printed layer can impede proper adhesion with the subsequently deposited layer.[53,54] In bi-layered configurations, TPU is printed directly onto the printer platform. In contrast, tri-layer configurations involve the deposition of a rigid polymer (PMMA or HIPS) atop an

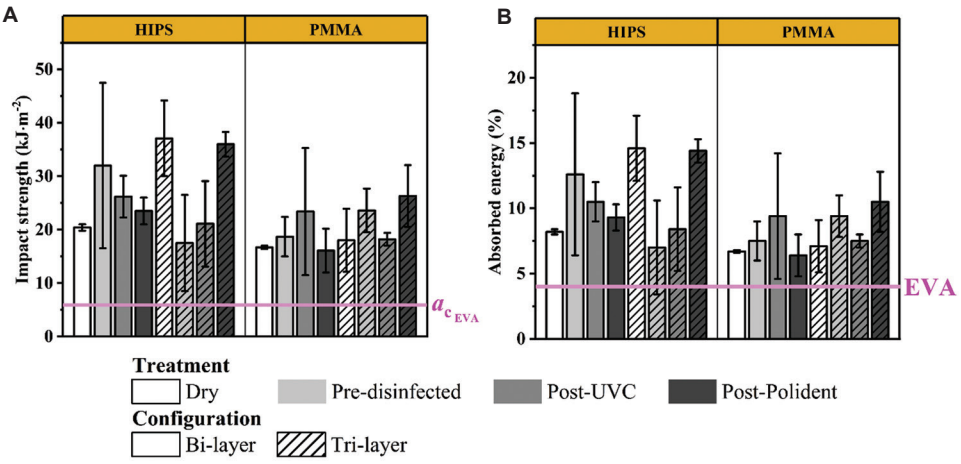

Figure 8. Charpy impact properties of 3D-printed multi-material parts. (A) Impact strength and (B) absorbed energy for bi-layered and tri-layered configurations. The pre-disinfected group includes specimens immersed in artificial saliva without further treatment. For reference, the impact strength and absorbed energy of bulk poly(ethylene-vinyl acetate) (EVA; pink) demonstrated an impact strength of 5.7 ± 0.5 kJ·m^{-2} and absorbed energy of 4.5 ± 0.4%

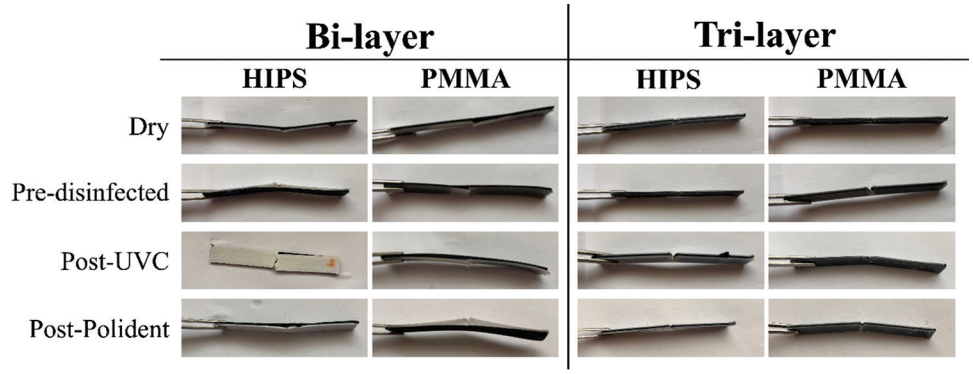

Figure 9. Macrographs of 3D-printed specimens after the transverse impact test. Delamination at the material interface is clearly visible in bi-layered configurations for both high-impact polystyrene (HIPS)- and poly(methyl methacrylate) (PMMA)-based parts across all treatment conditions (dry state, pre-disinfected [immersion in artificial saliva with no further disinfection], post-UVC, and post-Polident)

intermediate TPU layer. This additional interface likely promotes higher cohesion between layers in the tri-layered configuration, as compared to the direct TPU–platform adhesion in bi-layered parts. Furthermore, delamination was more pronounced in PMMA-based specimens, likely due to the weaker interfacial bonding between PMMA and TPU. This is consistent with the literature regarding poor compatibility between these two polymers.[53,54]

Ultimately, when comparing the tested multi-material configurations with conventional bulk EVA, it was found that EVA exhibits lower impact resilience and energy absorption capacity during transverse impact testing than all evaluated 3D-printed specimens.

3.4. Surface characterization

3.4.1. Vickers microhardness

Microhardness experiments were conducted to assess the Vickers hardness (HV) values of the printed specimens. Since both disinfection methods (UVC radiation and Polident solution) directly affect the surface of 3D-printed parts, assessing surface mechanical properties is important to understanding their impact on the overall mechanical behavior. A load of 50 g ($HV^{0.05}$, equivalent to 490 mN) was applied, and the results are presented in Figure 10.

The results indicate that the bi-layer configuration (represented by solid lines in Figure 10) exhibits higher average hardness values than the tri-layer configuration (dashed lines) for both materials. This outcome is likely due to the greater thickness of the more rigid material (HIPS or PMMA) in the bi-layered specimens, as supported by literature,[11] resulting in enhanced resistance to plastic deformation compared to tri-layered specimens. Furthermore, specimens comprising HIPS (black solid and dashed lines) showed consistently higher hardness values than those composed of PMMA (red solid and dashed lines). This finding is in accordance with the flexural modulus

results (Figure 7), which demonstrated that PMMA-based specimens are more prone to plastic deformation than their HIPS counterparts. An exception was observed in the tri-layered configuration under dry state, where PMMA-based specimens (14.8 ± 7.8 $HV^{0.05}$) exhibited greater HV compared to those made of HIPS (10.3 ± 5.2 $HV^{0.05}$), likely due to the higher standard deviations.

Regarding the effect of disinfection methods, the resistance to plastic deformation exhibited material- and configuration-dependent trends. For bi-layered configurations, UVC radiation increased hardness by approximately 40% and 38% for HIPS and PMMA, respectively, with no significant differences observed among the other groups (dry state, pre-disinfected, and post-Polident). In contrast, for tri-layered configurations, disinfection significantly increased hardness: UVC treatment led to increases of ~69% (HIPS) and ~10% (PMMA), whereas post-Polident treatment produced even greater enhancements—~107% (HIPS) and ~77% (PMMA). Although these findings suggest that both chemical and physical disinfection treatments can enhance surface hardness, the results should be interpreted with caution due to the relatively large standard deviations.

As discussed previously, disinfection methods may disrupt the surface chemical bonds of the polymeric materials, facilitating interactions between artificial saliva constituents and the polymer chains. These chemical interactions could reorganize surface functional groups, potentially leading to the formation of unsaturated bonds and altering the material's hardness.[17,52]

Therefore, a mouthguard with a surface that is more resistant to plastic deformation is expected to better mitigate damage propagation. Given its superior resistance to impact-induced deformation, the bi-layer HIPS configuration represents a promising approach for mouthguard fabrication. Nevertheless, the comprehensive mechanical test results indicate that the tri-layer configuration represents the optimal choice.

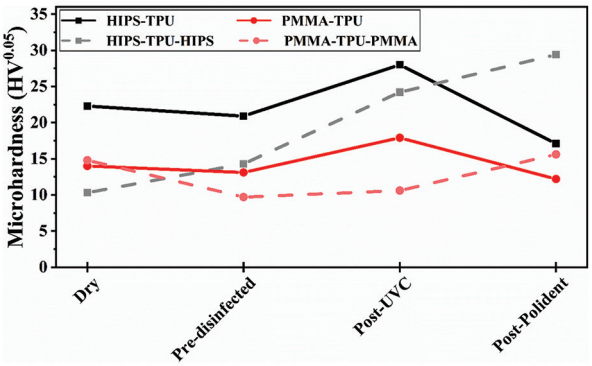

Figure 10. Mean values of microhardness measured under a 50 g load. The effect of disinfection is compared with the pre-disinfected group (immersed in artificial saliva but not subsequently disinfected). The dry state group serves as the negative control. Standard deviations are approximately 10% of the mean values (not shown)
Abbreviations: HIPS: High-impact polystyrene; PMMA: Poly(methyl methacrylate); TPU: Thermoplastic polyurethane

3.4.2. Wettability

Surface topography was analyzed to calculate the *r factor* (defined as the ratio between the true surface area and the projected surface area), the average surface roughness (S_a), and the quadratic surface roughness (S_q). The surface parameters of the 3D-printed specimens are presented in Table 4.

Despite the large standard deviations, HIPS generally exhibited higher roughness values than PMMA. Another interesting finding is that the *r factor* of bi-layered configurations is nearly twice that of the tri-layered configurations. This result may be due to the surface on which roughness was measured: the TPU layer in bi-layered specimens versus a non-TPU surface in tri-layered ones.

The wettability of the printed specimens was evaluated by measuring the contact angle between a water droplet and the specimen surface. According to Vogler,[55] biomaterials with contact angles below 65° in water are classified as hydrophilic.

However, surface roughness can influence the contact angle.[11,55] Therefore, the measured contact angle was corrected using Wenzel's equation. Figure 11 presents the corrected contact angles (θ_r) for each surface tested with distilled water.

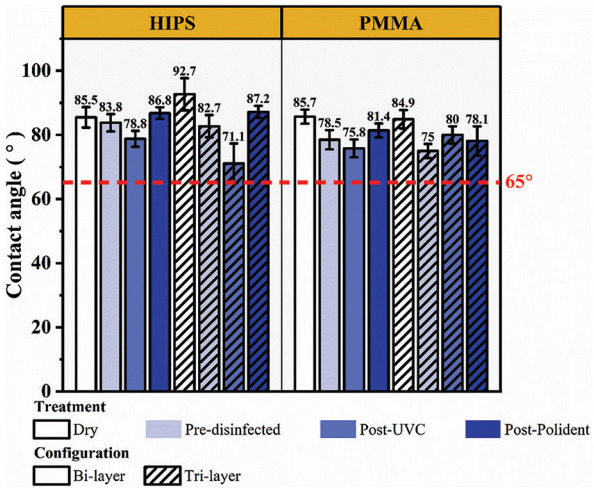

Figure 11. Corrected average contact angle values of the studied surfaces in contact with distilled water. 65° value is depicted (dashed red line) as the reference hydrophilicity criteria
Abbreviations: HIPS: High-impact polystyrene; PMMA: Poly(methyl methacrylate)

Table 4. Roughness parameters of the printed samples

Material	Configuration	Treatment	*r factor* (μm)	S_a (μm)	S_q (μm)
HIPS	Bi-layered configuration	Dry	6.0±0.7	27.7±2.7	35.5±2.9
		Pre-disinfected	4.5±2.3	27.5±5.9	35.0±6.5
		Post-UVC	4.8±1.2	28.5±9.5	35.4±10.4
		Post-Polident	5.0±1.2	31.8±6.1	37.7±6.2
	Tri-layered configuration	Dry	3.7±0.8	26.4±6.9	32.3±9.0
		Pre-disinfected	2.7±0.3	20.4±2.6	25.0±3.0
		Post-UVC	2.0±0.4	14.6±6.6	18.6±8.0
		Post-Polident	2.9±0.8	24.0±2.2	29.3±2.7
PMMA	Bi-layered configuration	Dry	4.1±0.4	22.8±4.9	28.8±5.4
		Pre-disinfected	3.9±0.6	27.5±2.6	33.2±3.3
		Post-UVC	3.3±1.4	19.7±5.0	25.8±5.6
		Post-Polident	3.9±0.8	24.5±3.4	30.1±3.1
	Tri-layered configuration	Dry	1.8±0.4	19.5±7.3	26.0±10.0
		Pre-disinfected	2.0±0.6	21.4±6.7	27.3±7.8
		Post-UVC	2.9±0.8	19.9±4.4	24.5±5.5
		Post-Polident	2.6±0.5	26.7±3.2	31.3±3.9

Abbreviations: HIPS: High-impact polystyrene; PMMA: Poly (methyl methacrylate).

All tested configurations exhibited hydrophobic behavior, consistent with prior findings.[11] The wettability of the materials is an important parameter, as saliva accumulation on the mouthguard surface can promote bacterial proliferation within the device.[17] For applications involving contact with tissues or cells, a material is considered hydrophilic when the contact angle with a water droplet is <65°.[55]

A comparison between the tested materials revealed that HIPS surfaces exhibited a slightly more hydrophobic character than PMMA, although the differences were not statistically significant.

As expected, specimens in the dry state demonstrated a more pronounced hydrophobic character – indicated by higher θ_r values – for both materials and configurations. This may be attributed to the sorption of ionic compounds following immersion in artificial saliva, which increases surface cohesion and improves wettability, thereby reducing resistance to wetting.[17,55]

Overall, specimens disinfected with UVC exhibited a lower degree of hydrophobicity compared to those treated with Polident. UV radiation likely induces chemical bond disruption and surface degradation,[52,56] which in turn alters surface roughness parameters and facilitates the spreading of water droplets. Nevertheless, despite this reduction in hydrophobicity, the corrected contact angle remains above 65°, indicating that the UVC disinfection method does not significantly contribute to saliva accumulation on the mouthguard surface.[11,55]

4. Conclusion

The main goal of this study was to investigate the mechanical properties of two multi-material configurations for the fabrication of customized mouthguards using additive manufacturing, particularly via FFF technology. More specifically, the study evaluated the effects of two disinfection methodologies – physical (UVC) and chemical (Polident solution) – on mechanical properties.

The results demonstrated that the disinfection process significantly influenced the mechanical properties of the printed components, as evidenced by three-point bending and microhardness tests.

Characterization demonstrated that HIPS exhibited higher values of flexural modulus, absorbed energy, and impact strength, whereas PMMA displayed greater flexural strength. Among the configurations tested, the tri-layered structure emerged as the optimal option for protective mouthguard fabrication, owing to its reduced susceptibility to damage and superior mechanical properties, including higher values of ,, absorbed energy, and impact strength.

Notably, the findings also indicate that the thickness of the mouthguard can be reduced while still improving its mechanical properties compared to 4 mm-thick bulk EVA. This reduction in thickness can diminish the discomfort experienced by athletes during use, while still ensuring effective impact protection.

Based on the obtained results, the most suitable material combination for additive manufacturing of mouthguards is HIPS–TPU–HIPS, which achieved ~35% improvement in the evaluated mechanical properties. This conclusion is supported by evidence showing that this multi-material configuration more effectively reduces, dissipates, and redistributes impact energy.

Acknowledgments

The authors would like to acknowledge the Portuguese Foundation for Science and Technology (Fundação para a Ciência e a Tecnologia [FCT]) through the Research Centre CEMMPRE, under project UIDB/00285.

Funding

Joana F. Henriques and Ana M. Sousa acknowledge financial support from FCT, Portugal, through the PhD grants 2023.00752.BD and UI/BD/150913/2020, respectively.

Conflicts of interest

Ana P. Piedade serves as the Editorial Board Member of the journal but did not in any way involved in the editorial and peer-review process conducted for this paper, directly or indirectly. Other authors declare they have no competing interests.

Authors' contributions

Conceptualization: Ana M. Sousa
Formal analysis: Leonor Bispo, Joana F. Henriques
Funding acquisition: Ana P. Piedade, Ana M. Sousa
Investigation: Leonor Bispo, Joana F. Henriques
Methodology: Leonor Bispo
Project administration: Ana P. Piedade, Ana M. Sousa
Resources: Ana P. Piedade
Supervision: Ana P. Piedade, Ana M. Sousa
Validation: Ana P. Piedade, Ana M. Sousa
Visualization: Leonor Bispo
Writing – original draft: Leonor Bispo, Joana F. Henriques
Writing – review and editing: Leonor Bispo, Joana F. Henriques, Ana P. Piedade, Ana M. Sousa

Ethics approval and consent to participate

Not applicable.

Consent for publication

Not applicable.

Availability of data

Data supporting this study are included within the article.

References

1. Zaman I, Rozlan SAM, Manshoor B, Ngali MZ, Khalid A, Amin NAM. Study of mouthguard design for endurance and air-flow intake. *IOP Conf Ser Mater Sci Eng*. 2017;226:012007.

   doi: 10.1088/1757-899X/226/1/012007

2. Singarapu R, Panneerselvam E, Balasubramaniam S, Nakkeeran KP, Ramanathan M, Raja VBK. The role of mouthguards in preventing temporomandibular joint injuries during contact sports: A prospective study. *Front Dent*. 2023;20:12.

   doi: 10.18502/fid.v20i12.12661

3. Lieger O, Von Arx T. Orofacial/cerebral injuries and the use of mouthguards by professional athletes in Switzerland. *Dent Traumatol*. 2006;22(1):1-6.

   doi: 10.1111/j.1600-9657.2006.00328.x

4. Knapik JJ, Marshall SW, Lee RB, *et al*. Mouthguards in sport activities: History, physical properties and injury prevention effectiveness. *Sports Med*. 2007;37(2):117-144.

   doi: 10.2165/00007256-200737020-00003

5. ASTM. *ASTM F697-16. Standard Practice for Care and Use of Athletic Mouth Protectors*. Available from: https://store.astm.org/f0697-16.html [Last accessed on 2025 Mar 14].

6. Green JI. The role of mouthguards in preventing and reducing sports-related trauma? *Prim Dent J*. 2017;6(2):27-34.

   doi: 10.1308/205016817821281738

7. Mantri SS, Mantri SP, Deogade S, Bhasin AS. Intra-oral mouth-guard in sport related Oro-facial injuries: Prevention is better than cure! *J Clin Diagn Res*. 2014;8:299-302.

   doi: 10.7860/JCDR/2014/6470.3872

8. ADA Council on Access, Prevention and Interprofessional Relations, ADA Council on Scientific Affairs. Using mouthguards to reduce the incidence and severity of sports-related oral injuries. *J Am Dent Assoc*. 2006;137(12):1712-1720; quiz 1731.

   doi: 10.14219/jada.archive.2006.0118

9. Parker K, Marlow B, Patel N, Gill DS. A review of mouthguards: Effectiveness, types, characteristics and indications for use. *Br Dent J*. 2017;222(8):629-633.

   doi: 10.1038/sj.bdj.2017.365

10. Guérard S, Barou JL, Petit J, Poisson P. Characterization of mouthguards: Impact performance. *Dent Traumatol*. 2017;33(4):281-287.

    doi: 10.1111/edt.12329

11. Sousa AM, Pinho AC, Piedade AP. Mechanical properties of 3D printed mouthguards: Influence of layer height and device thickness. *Mater Des*. 2021;203:109624.

    doi: 10.1016/j.matdes.2021.109624

12. Patrick DG, Van Noort R, Found MS. Scale of protection and the various types of sports mouthguard. *Br J Sports Med*. 2005;39(5):278-281.

doi: 10.1136/bjsm.2004.012658

13. Roberts HW. Sports mouthguard overview: Materials, fabrication techniques, existing standards, and future research needs. *Dent Traumatol*. 2023;39(2):101-108.

doi: 10.1111/edt.12809

14. Maeda Y, Kumamoto D, Yagi K, Ikebe K. Effectiveness and fabrication of mouthguards. *Dent Traumatol*. 2009;25(6):556-564.

doi: 10.1111/j.1600-9657.2009.00822.x

15. Coto NP, Brito e Dias R, Costa RA, Antoniazzi TF, Carvalho EPC. Mechanical behaviour of ethylene vinyl acetate copolymer (EVA) used for manufacture mouthguards and interocclusal splints. *Braz Dent J*. 2007;18(4):324-328.

doi: 10.1590/S0103-64402007000400010

16. Almeida MH, Ceschim GV, Iorio NLPP, *et al*. Influence of thickness, colour, and polishing process of ethylene-vinyl-acetate sheets on surface roughness and microorganism adhesion. *Dent Traumatol*. 2018;34(1):51-57.

doi: 10.1111/edt.12374

17. Li C, Wada T, Tsuchida Y, *et al*. Optimizing additively manufactured mouthguards: An evaluation of multi-layer materials for improved shock absorption and durability compared to conventionally fabricated samples. *Int J Bioprint*. 2024;10:2469.

doi: 10.36922/ijb.2469

18. Bandyopadhyay A, Heer B. Additive manufacturing of multi-material structures. *Mater Sci Eng R Rep*. 2018;129:1-16.

doi: 10.1016/j.mser.2018.04.001

19. Unkovskiy A, Huettig F, Kraemer-Fernandez P, Spintzyk S. Multi-material 3D printing of a customized sports mouth guard: Proof-of-concept clinical case. Int J Environ Res Public Health. 2021;18:12762.

doi: 10.3390/ijerph182312762

20. Ribeiro YJS, Delgado RZR, Paula-Silva FWG, *et al*. Sports mouthguards: Contamination, roughness, and chlorhexidine for disinfection - a randomized clinical trial. *Braz Dent J*. 2021;32(6):66-73.

doi: 10.1590/0103-6440202104533

21. Hayran Y, Sarikaya I, Aydin A, Tekin YH. Determination of the effective anticandidal concentration of denture cleanser tablets on some denture base resins. *J Appl Oral Sci*. 2018;26:e20170077.

doi: 10.1590/1678-7757-2017-0077

22. Bae CH, Lim YK, Kook JK, Son MK, Heo YR. Evaluation of antibacterial activity against *Candida albicans* according to the dosage of various denture cleansers. *J Adv Prosthodont*. 2021;13(2):100-106.

doi: 10.4047/jap.2021.13.2.100

23. Hayashi H, Naiki Y, Murakami M, *et al*. Effects of cleaning sports mouthguards with ethylene-vinyl acetate on oral bacteria. *PeerJ*. 2022;10:e14480.

doi: 10.7717/peerj.14480

24. International Organization for Standardization. *ISO 10271:2020 Dental Metallic Materials Corrosion Test Methods*. Available from: https://www.iso.org/standard/73445.html [Last accessed on 2024 Dec 15].

25. Kechagias JD, Zaoutsos SP, Fountas NA, Vaxevanidis NM. Experimental investigation and neural network development for modeling tensile properties of polymethyl methacrylate (PMMA) filament material. *Int J Adv Manuf Tech*. 2024;134:4387-4398.

doi: 10.1007/s00170-024-14402-0

26. Kumar R, Singh R, Farina I. On the 3D printing of recycled ABS, PLA and HIPS thermoplastics for structural applications. *PSU Res Rev*. 2018;2(2):115-137.

doi: 10.1108/PRR-07-2018-0018

27. Sastri VR. Commodity thermoplastics: Polyvinyl chloride, polyolefins, cycloolefins and polystyrene. In: Sastri VR, editors. *Plastics in Medical Devices*. 3rd ed. Elsevier; 2022. p. 113-166.

doi: 10.1016/B978-0-323-85126-8.00002-3

28. Gong XH, Tang CY, Hu HC, Zhou XP, Xie XL. Improved mechanical properties of HIPS/hydroxyapatite composites by surface modification of hydroxyapatite via in-situ polymerization of styrene. *J Mater Sci Mater Med*. 2004;15:1141-1146.

doi: 10.1023/B:JMSM.0000046397.09060.15

29. Al Nakib R, Toncheva A, Fontaine V, Vanheuverzwijn J, Raquez J, Meyer F. Thermoplastic polyurethanes for biomedical application: A synthetic, mechanical, antibacterial, and cytotoxic study. *J Appl Polym Sci*. 2022;139:e51666.

doi: 10.1002/app.51666

30. Prajapati S, Sharma JK, Kumar S, Pandey S, Pandey MK. *A Review on Comparison of Physical and Mechanical Properties of PLA, ABS, TPU, and PETG Manufactured Engineering Components by using Fused Deposition Modelling*. Netherlands: Elsevier; 2024.

doi: 10.1016/j.matpr.2024.05.018

31. Ali U, Abd Karim KJB, Buang NA. A review of the properties and applications of poly (Methyl Methacrylate) (PMMA). *Polym Rev*. 2015;55:678-705.

doi: 10.1080/15583724.2015.1031377

32. Amirabad LM, Tahriri M, Zarrintaj P, Ghaffari R, Tayebi L. Preparation and characterization of TiO2-coated polymerization of methyl methacrylate (PMMA) for biomedical applications: *In vitro* study. *Asia Pac J Chem Eng*. 2022;17:e2761.

    doi: 10.1002/apj.2761

33. Lopes LR, Silva AF, Carneiro OS. Multi-material 3D printing: The relevance of materials affinity on the boundary interface performance. *Addit Manuf*. 2018;23:45-52.

    doi: 10.1016/j.addma.2018.06.027

34. ASTM. *ASTM D790-03: Standard Test Method for Flexural Properties of Unreinforced and Reinforced Plastics and Electrical Insulation Materials*. Available from: https://cdn.standards.iteh.ai/samples/27059/f08b79ad9a784319871f02f70e5b399a/astm-d790-03.pdf [Last accessed on 2025 Jan 13].

35. Boisse P, Colmars J, Hamila N, Naouar N, Steer Q. Bending and wrinkling of composite fiber preforms and prepregs. A review and new developments in the draping simulations. *Compos Part B Eng*. 2018;141:234-249.

    doi: 10.1016/j.compositesb.2017.12.061

36. Kumar A, Venkatappa Rao T, Ray Chowdhury S, Ramana Reddy SVS. Compatibility confirmation and refinement of thermal and mechanical properties of poly (lactic acid)/poly (ethylene-co-glycidyl methacrylate) blend reinforced by hexagonal boron nitride. *React Funct Polym*. 2017;117:1-9.

    doi: 10.1016/j.reactfunctpolym.2017.05.005

37. International Organization for Standardization. *ISO 179-1:2023 Determination of Charpy impact properties. Part 1: Non instrumented impact test*. Available from: https://www.iso.org/standard/84393.html [Last accessed on 2025 Jan 15].

38. International Organization for Standardization. *ISO 6507-1:2023 Metallic materials-Vickers Hardness Test*. Available from: https://www.iso.org/standard/83898.html [Last accessed on 2025 Jan 13].

39. Deng Y, Peng C, Dai M, *et al*. Recent development of super-wettable materials and their applications in oil-water separation. *J Clean Prod*. 2020;266:121624.

    doi: 10.1016/j.jclepro.2020.121624

40. Nituica M, Oprea O, Stelescu MD, *et al*. Polymeric bio composite based on thermoplastic polyurethane (TPU) and protein and elastomeric waste mixture. *Materials*. 2023;16:5279.

    doi: 10.3390/ma16155279

41. Arash S, Akbari B, Ghaleb S, Kaffashi B, Marouf BT. Preparation of PLA-TPU-nanoclay composites and characterization of their morphological, mechanical, and shape memory properties. *J Mech Behav Biomed Mater*. 2023;139:105642.

    doi: 10.1016/j.jmbbm.2022.105642

42. Calvo-Correas T, Benitez M, Larraza I, Ugarte L, Peña-Rodríguez C, Eceiza A. Advanced and traditional processing of thermoplastic polyurethane waste. *Polym Degrad Stab*. 2022;198:109880.

    doi: 10.1016/j.polymdegradstab.2022.109880

43. Giakoumakis NS, Vos C, Janssens K, *et al*. Total revalorization of high impact polystyrene (HIPS): Enhancing styrene recovery and upcycling of the rubber phase. *Green Chem*. 2024;26(1):340-352.

    doi: 10.1039/D3GC02407E

44. Thanh Truc NT, Lee BK. Combining ZnO/microwave treatment for changing wettability of WEEE styrene plastics (ABS and HIPS) and their selective separation by froth flotation. *Appl Surf Sci*. 2017;420:746-752.

    doi: 10.1016/j.apsusc.2017.04.075

45. Sekhar VC, Nampoothiri KM, Mohan AJ, Nair NR, Bhaskar T, Pandey A. Microbial degradation of high impact polystyrene (HIPS), an e-plastic with decabromodiphenyl oxide and antimony trioxide. *J Hazard Mater*. 2016;318:347-354.

    doi: 10.1016/j.jhazmat.2016.07.008

46. Elashmawi IS, Hakeem NA. Effect of PMMA addition on characterization and morphology of PVDF. *Polym Eng Sci*. 2008;48(5):895-901.

    doi: 10.1002/pen.21032

47. Huszank R, Szilágyi E, Szoboszlai Z, Szikszai Z. Investigation of chemical changes in PMMA induced by 1.6 MeV He^+ irradiation by ion beam analytical methods (RBS-ERDA) and infrared spectroscopy (ATR-FTIR). *Nucl Instrum Methods Phys Res B Beam Interact Mater Atoms*. 2019;450:364-368.

    doi: 10.1016/j.nimb.2018.05.016

48. Aziza SB, Abdullaha OG, Brzac MA, Azawyd AK, Tahir DA. Effect of carbon nano-dots (CNDs) on structural and optical properties of PMMA polymer composite. *Results Phys*. 2019;15:102776.

    doi: 10.1016/j.rinp.2019.102776

49. Ramesh S, Leen KH, Kumutha K, Arof AK. FTIR studies of PVC/PMMA blend based polymer electrolytes. *Spectrochim Acta A Mol Biomol Spectrosc*. 2007;66(4-5):1237-1242.

    doi: 10.1016/j.saa.2006.06.012

50. O'Toole GA. Classic spotlight: Plate counting you can count on. *J Bacteriol*. 2016;198:3127.

    doi: 10.1128/JB.00711-16

51. Cummins NK, Spears IR. The effect of mouthguard design on stresses in the tooth-bone complex. *Med Sci Sports Exerc*. 2002;34(6):942-947.

    doi: 10.1097/00005768-200206000-00006

52. Amza CG, Zapciu A, Baciu F, Radu C. Effect of UV-C radiation on 3D printed ABS-PC polymers. *Polymers*

(Basel). 2023;15:1966.

doi: 10.3390/polym15081966

53. Brischetto S, Ferro CG, Torre R, Maggiore P. 3D FDM production and mechanical behavior of polymeric sandwich specimens embedding classical and honeycomb cores. *Curved Layer Struct*. 2018;5(1):80-94.

doi: 10.1515/cls-2018-0007

54. Głowacki M, Mazurkiewicz A, Słomion M, Skórczewska K. Resistance of 3D-printed components, test specimens and products to work under environmental conditions-review. *Materials*. 2022;15:6162.

doi: 10.3390/ma15176162

55. Piedade AP, Nunes J, Vieira MT. Thin films with chemically graded functionality based on fluorine polymers and stainless steel. *Acta Biomat*. 2008;4(4):1073-1080.

doi: 10.1016/j.actbio.2008.02.023

56. Yousif E, Haddad R. Photodegradation and photostabilization of polymers, especially polystyrene: Review. *SpringerPlus*. 2013;2:398.

doi: 10.1186/2193-1801-2-398